

## Evolution of aseismic slip rate along plate boundary faults before and after megathrust earthquakes

Toshihiro Igarashi <sup>1</sup>✉ & Aitaro Kato <sup>1</sup>

Similar earthquakes that occur in approximately the same location have the potential to reveal the spatio-temporal changes in aseismic slip along plate boundaries. Here we identify similar earthquakes with moderate magnitudes that occurred worldwide between 1989 and 2016 by using seismograms recorded by the Japanese dense seismic network. The slip rate along the plate boundaries estimated from similar earthquakes increased rapidly following  $M > 8$  megathrust ruptures and then gradually decayed over periods of ~10 years, which correlates with after-slip progressing around the source areas. More than 30 years after large megathrust earthquakes, the slip rate begins to show a gradual increase. This gradual increase in slip rate after the decay may be due to an increase in stress levels that accumulate during tectonic loading. The spatio-temporal characteristics of inter-plate aseismic slip can be used to provide a valuable framework for understanding the long-term evolution of slip-rate during megathrust earthquake cycles.

<sup>1</sup>Earthquake Research Institute, the University of Tokyo, Tokyo, Japan. ✉email: [igarashi@eri.u-tokyo.ac.jp](mailto:igarashi@eri.u-tokyo.ac.jp)

An earthquake is a sudden fast slip event that propagates dynamically along a fault and releases elastic energy accumulated due to a locking of the fault during the inter-seismic period. Growing evidence of geophysical observations has demonstrated that subduction zone faults host a broad spectrum of slip modes, from slow to fast slip<sup>1,2</sup>. This recent view is quite different from the classic notion of allowing only two discrete states of fault: locking and fast slip.

Earthquakes with similar waveforms are typically considered to occur at approximately the same location but at different times, and are referred to as similar earthquakes. Seismic observations made over several decades in Japan have shown that many similar earthquake sequences in the subducting plates are caused by repeated slips in small patches surrounded by creeping aseismic regions along with the plate boundary<sup>3–5</sup>. These sequences are also referred to as repeating earthquakes due to the recurring nature of seismic energy release, and they yield information on the spatio-temporal evolution of fault slip rate (i.e., creeping rate).

Recently, similar earthquakes have been detected in many regions around the world, based on similarities in seismogram characteristics and the inter-event distance of each earthquake pair. This includes subducting plate boundaries in Japan<sup>4</sup>, the Kuril–Kamchatka–Aleutian Islands, and the South Sandwich Islands<sup>6</sup>, the Tonga–Fiji–Solomon region<sup>6,7</sup>, Sumatra<sup>8</sup>, and Chile<sup>9,10</sup>. In addition, similar earthquakes have been detected in the plate collision zone in Taiwan<sup>11</sup>, along with transform faults in California<sup>12</sup>, from plate interiors<sup>13–19</sup>, in mines<sup>20</sup>, and at intermediate-deep depths in subducting slabs<sup>6,21</sup>.

The recurrent nature of similar earthquakes over relatively long periods of time can be used to directly analyze spatio-temporal changes in slip rate along inter-plate boundaries at depth<sup>4</sup>. This is normally difficult to achieve from surface geodetic measurements, especially in offshore regions that contain few geodetic stations. In addition, changes in seismogram characteristics at the time of recurrence can be used to investigate temporal changes in seismic velocity within the Earth<sup>22,23</sup>. In this study, we detected moderate-sized similar earthquakes around the world by calculating the cross-correlation coefficients of bandpass-filtered seismograms recorded by the Japanese dense seismic network. Based on these data, we investigated the spatial distributions and temporal characteristics of inter-plate aseismic slip at a number of subduction zones around the world.

## Results

**Spatial distribution of similar earthquakes.** We used seismic waveform data collected by dense nationwide seismic networks located across the Japanese islands (Fig. 1). To extract similar earthquakes, we calculated the cross-correlation coefficient of the vertical component in bandpass-filtered seismograms at each station (see ‘Methods’). The hemisphere map centered on Japan in Fig. 1 shows the distribution of the cross-correlation coefficients obtained in this study. We identified numerous similar earthquakes that occurred along subducting plate boundaries, including the Andaman–Sumatra–Java, the Solomon–Vanuatu–Tonga, and Japan–Kuril–Kamchatka–Aleutian subduction zones. These similar earthquakes are linked to aseismic fault slip along shallow inter-plate boundaries at depths of <100 km. The similar earthquakes are distributed heterogeneously, even within single subduction zones that host megathrust earthquakes. Similar earthquakes were also identified at depths of >100 km in regions where intra-slab earthquakes occur frequently (e.g., the Solomon, Tonga, and Izu–Ogasawara regions). These deeper events might have been detected due to relatively simple source processes, the relatively homogeneous structure near the source, and a nearly identical path to radiated seismic waves.

In contrast, similar earthquakes were not detected in China, although previous studies have identified pairs of similar events in this region<sup>14</sup>. The contrasting results of the present and previous studies may have been caused by a difference in the analyzed seismic phase and frequency band.

**Average slip rate along the subducting plate boundary.** Based on the spatio-temporal evolutions of similar earthquakes that occurred during the analysis period, we demonstrate that inter-plate similar earthquake sequences occurred more frequently after megathrust earthquakes. Other sequences of similar earthquakes have a constant recurrence interval of several years to several decades. Pairs of similar earthquakes with the longest recurrence interval (~20 years) occurred in the Aleutian Islands. These sequences may reflect spatio-temporal changes in inter-plate aseismic slip, and we, therefore, attempt to analyze such changes in subduction zones around the Pacific and Indian oceans based on similar earthquakes extracted in this study.

To estimate the aseismic slip history, we assume that the slip rate during the inter-seismic period of similar earthquake sequences is equal to the slip rate of surrounding creeping areas (see ‘Methods’). If the moderate-sized similar earthquakes analyzed in this study have recurrence intervals that relate to the plate convergence rate, the recurrence interval at the plate boundaries with low average slip rates will exceed 10 years. The resolvable lower limit of the slip rate that can be estimated from the similar earthquakes in the 27-year interval used in this study is about 20–30 mm yr<sup>-1</sup>, depending on the recurrence time and magnitude of the similar earthquakes.

Figure 2a shows the average slip rates in subduction zones estimated from similar earthquakes that occurred at depths of <100 km. The average slip rates vary laterally between different subduction zones, and in some cases along the length of the same subduction zone. Figure 2b shows the relationship between the relative velocity of the two converging plates, taking into account back-arc spreading<sup>24</sup>, the estimated slip rates in each region are shown in Fig. 2a. The estimated slip rates in several areas are higher than the relative velocity of the two converging plates. These areas correspond to regions in which postseismic slip has occurred recently following giant earthquakes, including the 2004 Sumatra–Andaman earthquake (*M*w9.1) in area 12, the 2005 northern Sumatra earthquake (*M*w8.6) in area 13, the 2006 Kuril earthquake (*M*w8.3) in area 2c, the 2007 southern Sumatra earthquake (*M*w8.4) in area 14, and the 2011 Tohoku–Oki earthquake (*M*w9.1) in area 2f. These areas show large error bars due to the spatio-temporal variation of the slip rates linked to the postseismic slip (Fig. 2b). The increase of slip rate in area 5 near the Kanto District in Japan was induced by the 2011 Tohoku–Oki earthquake<sup>25</sup>. The recurrence intervals of similar earthquake sequences decreased significantly following these recent giant earthquakes, resulting in an increase in the average slip rate.

In contrast, we recognized several areas where the slip rates are much lower than the relative plate velocities, including the Kuril–Kamchatka–Aleutian (areas 1–2), Nankai–Ryukyu (areas 6–7), Manila (area 9), Philippines (area 10), and Solomon (areas 16–20) subduction zones. These observations indicate that the plate boundary faults in these regions are strongly locked, and that elastic strain energy has been accumulating within each of these subduction zones.

Slip rates in some areas are almost equal to the rate of relative plate motion, including the northern extents of the 1952 and 2011 *M*9 earthquakes, the Izu–Bonin–Mariana region (areas 3–4), and parts of the Solomon subduction zone (areas 16–20). These regions may host episodic aseismic slip events, including slow slip events and/or creeping movement. The Tonga subduction zone

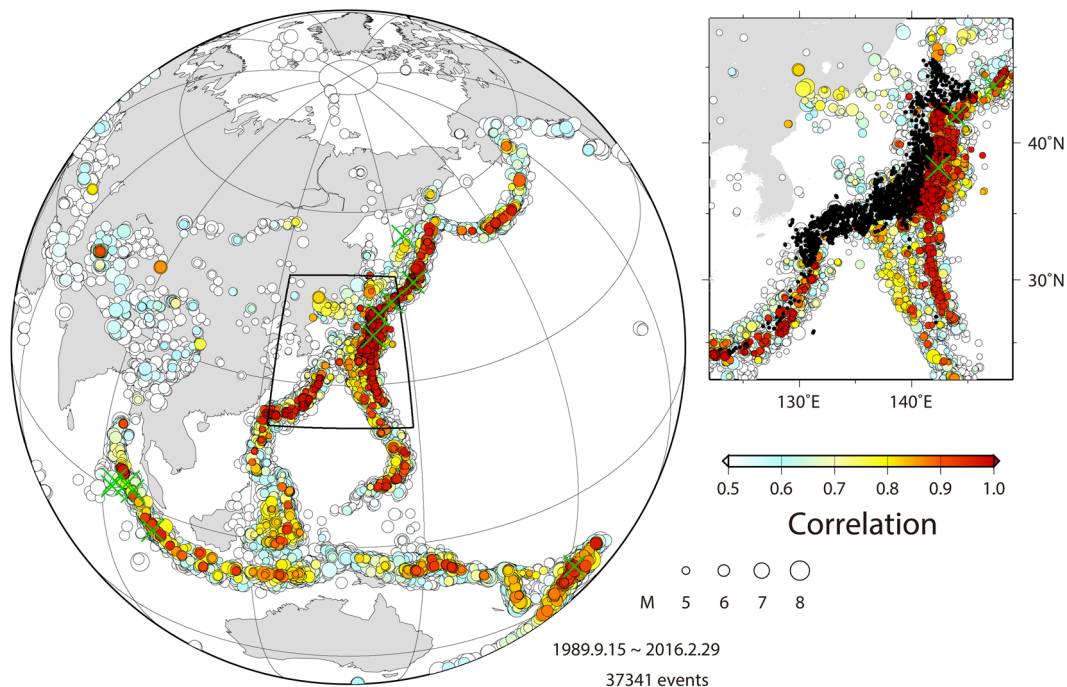


**Fig. 1 Distribution of epicenters analyzed in this study.** This map is shown on a hemisphere centered on Japan. The color scale shows the maximum cross-correlation coefficient for each event. The symbol size is proportional to magnitude, as shown in the legend. Green crosses show epicenters of  $M_w \geq 8.2$  earthquakes that occurred during the analysis period. The inset map shows an enlargement of the area around Japan. Black dots show the locations of seismic stations used in this study.

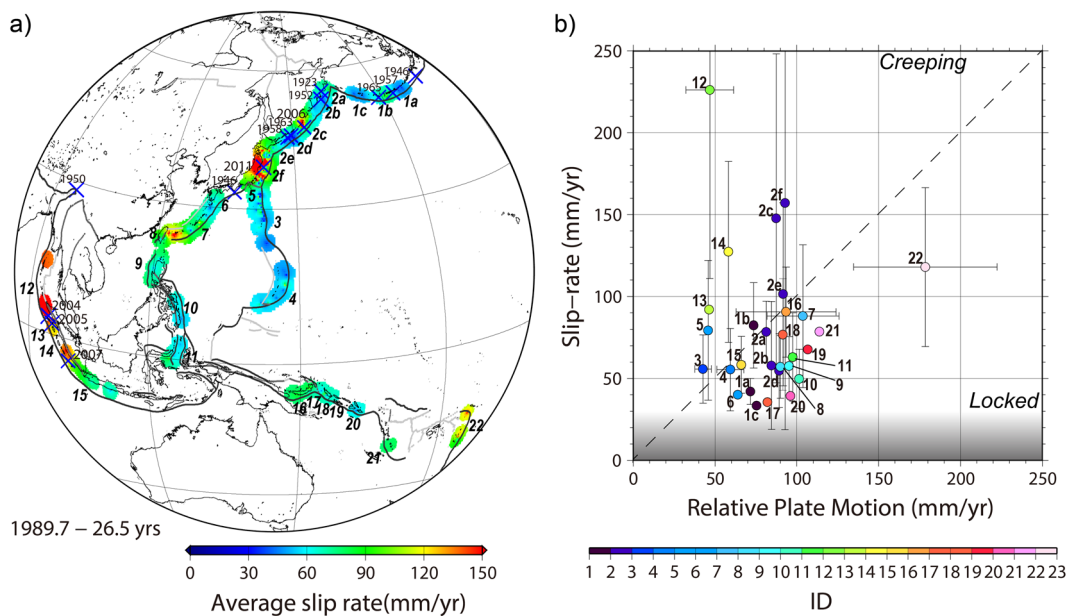


**Fig. 2 Estimated average slip rates in subduction zones.** **a** Distribution of average slip rates estimated from shallow similar earthquake sequences in subduction zones (during the period from 15 September 1989 to 29 February 2016). Crosses indicate the epicenters of  $M_w \geq 8.3$  inter-plate earthquakes after 1923. **b** Relationship between the relative plate velocity<sup>24</sup> and the estimated average slip rates for each region shown in **(a)**. The error bars represent their standard deviations. The slip rate can be determined above the gray shadow band ( $>20\text{--}30\text{ mm yr}^{-1}$ ).

(area 22) has a high rate of relative plate motion and also shows relatively high rates of fault slip. Back-arc spreading has occurred in the Ryukyu (area 7), Mariana (area 4), and Tonga (area 22) areas. The slip rates estimated from similar earthquakes are consistent with the relative velocities of plate motion, which includes the back-arc spreading rate.

These results suggest that the spatio-temporal changes in inter-plate aseismic slip in many areas around the world can be estimated

from similar earthquake sequences. It might not be possible to detect similar earthquakes in areas with slip rates lower than the detection threshold ( $20\text{--}30\text{ mm yr}^{-1}$ ). Previous studies have suggested that the source regions of large earthquakes show notable slip deficits during the inter-seismic period<sup>4</sup>. This period may be represented by some areas of the Aleutian (area 1), Kuril–Kamchatka (areas 2b, d), and Solomon–Vanuatu (areas 17, 19–21) subduction zones that are currently strongly locked.

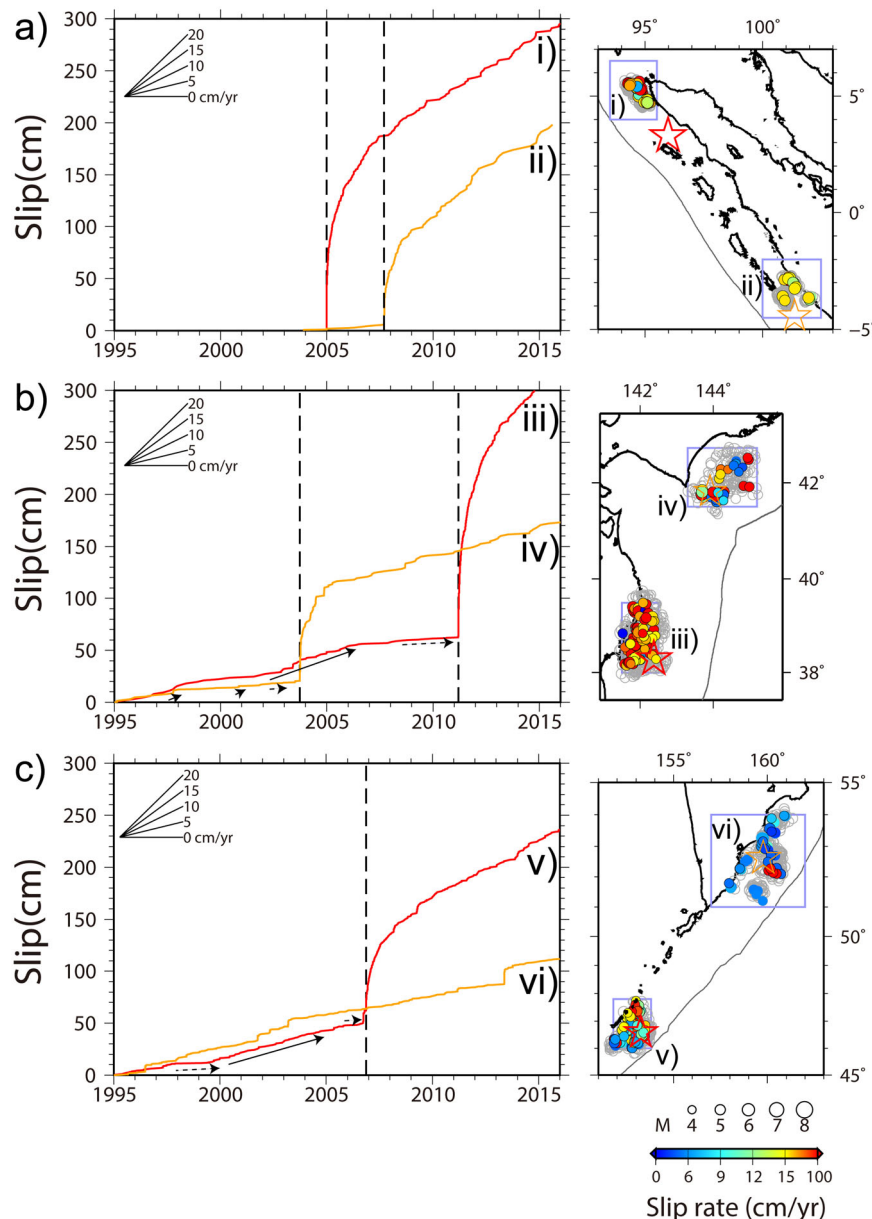


**Fig. 3 Short-term slip histories in areas near the hypocenters of megathrust earthquakes.** **a** the 2004 Sumatra–Andaman earthquake ( $M_w$ 9.1) and the 2007 southern Sumatra earthquake ( $M_w$ 8.4), **b** the 2011 Tohoku–Oki earthquake ( $M_w$ 9.1) and the 2003 Tokachi–Oki earthquake ( $M_w$ 8.2), and **c** the 2006 Kuril Islands earthquake ( $M_w$ 8.3, Earthquake v) and the 1952 Kamchatka earthquake ( $M_w$ 9.0, Earthquake vi). The slip rate is constrained by similar earthquakes and background seismicity. The solid and dashed arrows indicate the periods of increased or decreased slip rate, respectively. The maps show the locations of the analyzed areas. Colored symbols on maps show the slip rates estimated from each similar earthquake sequence. Gray circles are epicenters of analyzed  $M \geq 4.5$  earthquakes.

**Short-term history of slip rate.** The average slip rates shown in Fig. 2 indicate slip acceleration in source regions that have recently hosted megathrust earthquakes. However, the similar earthquakes have recurrence intervals of years to decades, which are too long to investigate temporal variations in short-term slip rates. To track such short-term variations, we compute “short-term slip rates” assuming that the slip rate of each recurring similar earthquake is perturbed according to temporal changes observed in the regular seismic activity in adjacent regions (see ‘Methods’).

Figure 3 shows the short-term histories in three areas near the hypocenters of the recent  $M$ 8–9 class megathrust earthquakes. Immediately after each megathrust earthquake, we detect clear afterslip in the source regions. The areas with afterslip coincide approximately with those estimated from geodetic data

analysis<sup>26–28</sup>, although it is not possible to detect all of the afterslip areas due to the limited occurrence of regional moderate-sized earthquakes. The duration of afterslip following  $M$ 8 class events was  $\sim 2$ –5 years. On the other hand, as of February 2016, the areas affected by the 2004 Sumatra–Andaman earthquake ( $M_w$ 9.1) and the 2011 Tohoku–Oki earthquake ( $M_w$ 9.1) had higher slip rates than the relative plate motions along each subduction boundary. The great earthquakes have a higher maximum slip rate and longer duration of afterslip. The estimated slip rate was highest in the western part of the epicentral area of the Tohoku–Oki earthquake, namely the down-dip side of the ruptured area. The amount of slip that occurred within an area of  $1.5^\circ$  by  $1.0^\circ$  was  $\sim 230$  cm over 3 years, which is consistent with estimates derived from geodetic data<sup>28</sup>.

## Discussion

The long-term trend in slip rates, measured over decadal scales, seems to increase several years before megathrust earthquakes (Fig. 3), indicating an unlocking of the plate boundary fault. Indeed, geodetic measurements made using onshore GNSS networks reveal that long-term aseismic creep on the plate interface had occurred down dip and to the south of the large coseismic slip zone of the 2011 Tohoku-Oki mainshock rupture<sup>29,30</sup>. Foreshock sequences including slow slip transients have been reported over timescales of several weeks immediately preceding the Tohoku-Oki earthquake<sup>31</sup>. In contrast, our result for the area near the epicenter (areas iii and v in Fig. 3) shows that the slip rates increased for about 5–8 years before the mainshock, but then tend to decrease ~1–3 years before them. Because the recurrence interval of similar earthquakes analyzed in this study (magnitude of  $\geq 4.5$ ) is longer than several years, it is difficult to determine the short-term temporal evolution of slip before megathrust earthquakes. To improve the temporal resolution of slip rate using this type of analysis, we require additional observational data on the waveform similarity of earthquakes with smaller magnitudes. Such an improved catalog would strengthen our understanding of the relationships between spatio-temporal changes in slip rate and megathrust earthquakes.

Nevertheless, the present catalog provides a valuable framework for understanding the long-term evolution of slip rate during the earthquake cycle. Figure 4 shows a time series analysis of stacked slip rates plotted against the elapsed time since the 11 megathrust earthquakes with  $M_w \geq 8.3$  that occurred after 1923. The slip rates calculated for each subduction zone were smoothed using a 3-year moving average, and normalized to the plate convergence rate in the area (see ‘Methods’). The analysis shows that following rupture of each earthquake, the slip rates initially increased rapidly and then gradually decayed over periods of ~10 years, which correlates with afterslip. After ~30 years, the slip rate begins to increase as we approach the next megathrust rupture (blue shaded curve in Fig. 4). This gradual increase in slip rate during the middle and later stages of the earthquake cycle may be due to an increase in stress levels that accumulate during tectonic loading. Numerical simulations of megathrust rupture show that

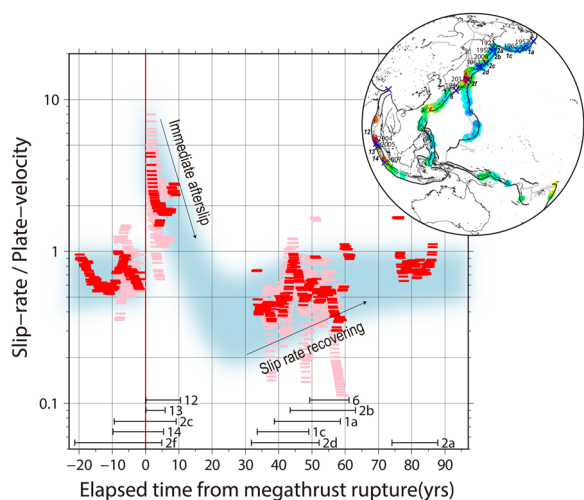


**Fig. 4 Relationship between the normalized slip rate and the elapsed time from megathrust earthquakes with  $M_w \geq 8.3$ .** Pink bars show slip rates aligned to the time of occurrence of each megathrust earthquake. Red bars are the stacked slip rates. The slip rates were smoothed using a 3-year moving average, and normalized by the plate convergence rate in each area. The blue curve outlines the long-term evolution of slip rate during the megathrust earthquake cycle.

aseismic sliding at a slip velocity of 30–60% of the plate convergence rate starts midway through the earthquake cycle and continues until megathrust rupture in the afterslip area where many similar earthquakes occur<sup>32</sup>. The local heterogeneity of slip rate within the source region may also contribute to the stress loading of the main locked area.

The absence of similar earthquakes in some areas during the analysis period suggests that such areas are either completely locked or experience quasi-static slip. Source regions of giant earthquakes that occurred before the analysis period, such as the 1952 Kamchatka earthquake, have large slip deficits. In regions where no similar earthquakes were detected but other regular earthquakes continued to occur, the slip rate is assumed to be extremely low. Areas that experienced large coseismic slips during megathrust earthquakes show very low numbers of regular earthquakes. This means that seismic potential can be assessed in previously ruptured areas or in regions that are surrounded by seismogenic areas. According to the time predictable model, an earthquake will occur when the amount of accumulated slip is equal to the slip during the previous large earthquake. Even if the slip predictable model is applied, the amount of slip produced by a potential earthquake can be estimated by tracking the cumulative slip deficit.

We believe that additional similar earthquakes will be detected by extending the analysis periods in areas where similar earthquakes were not identified in this study. A comparable analysis of small-magnitude earthquakes using local seismic networks could also be used to estimate inter-plate slip at a higher spatial and temporal resolution. A comprehensive database of local and global similar earthquakes would enable comparison of inter-plate aseismic slip characteristics along various plate boundary zones around the world. Furthermore, such a database could be used to extract information on spatio-temporal changes in the seismic velocity structures beneath seismic observation networks in Japan and around the world.

## Methods

**Data.** We used seismic waveform data collected by dense nationwide seismic networks located across the Japanese islands. The seismic networks have been operated consistently over several decades by the National Research Institute for Earth Science and Disaster Resilience (NIED), the Japan Meteorological Agency (JMA), and Earthquake Research Institute (ERI) at the University of Tokyo (Fig. 1). This represents the most suitable seismic observation network in the world in terms of detecting and analyzing the long-term activity of similar earthquakes. Using the worldwide hypocenter catalog of the United States Geological Survey, we focused on events with magnitudes of  $\geq 4.5$  at distances of  $< 90^\circ$  that occurred from 15 September 1989 to 29 February 2016. For each event, we selected waveform data with a high signal-to-noise ratio around the onset of the P-wave arrival. A total of 1340 seismic stations were available and 37,341 target events were analyzed.

**Extraction of similar earthquakes.** To extract similar earthquakes, we detected earthquake pairs with epicenter separations and differences in back azimuth of  $< 3^\circ$ . For each earthquake pair, we used the method of Igarashi<sup>4</sup> to calculate the cross-correlation coefficient of the vertical component in bandpass-filtered seismograms at each station. The time window used to compute cross-correlation coefficients was 80 s from the P-wave onset. We applied multiple bandpass filters to the waveforms, with passbands of 0.1–0.5, 0.2–1.0, 0.5–2.0, and 1.0–4.0 Hz, and computed the cross-correlation coefficient at each filter band. We chose the highest cross-correlation coefficient from those in the analyzed filter bands as a representative value for each station. The median of the correlation values over the nationwide seismic network was adopted as the cross-correlation coefficient of the earthquake pair, following Aster and Scott<sup>33</sup>.

Considering multiple sources of scattering during the propagation of seismic waves, the similarity of waveforms decreases exponentially with an increasing inter-event distance<sup>12,34</sup>. Thus, earthquakes sharing almost identical waveforms are considered to have occurred in nearly the same location. We identified similar earthquakes based only on waveform similarities, because we could not obtain information on the relative hypocenter locations that are needed to determine the overlapping source areas within each earthquake pair.

When the median of the cross-correlation coefficient from an earthquake pair exceeded 0.85, it was identified as a similar earthquake pair. This threshold was selected by comparison with the existing catalogs of similar earthquakes compiled

in the previous studies<sup>8</sup>. If several earthquake pairs shared the same event, they were grouped together as within the same sequences of similar earthquakes. A total of 3579 similar earthquakes (from 1125 sequences) that occurred over a 26 year period were extracted. The complete list of similar earthquakes is provided in Supplementary Data 1.

**Estimation of slip rate.** To estimate the aseismic slip history, we applied the method of Igarashi<sup>4</sup> to our catalog of similar earthquakes. This method assumes that the slip rate during the inter-seismic period of similar earthquake sequences is equal to the slip rate of surrounding creeping areas, which is calculated based on the amount of slip and the recurrence interval of each similar earthquake. The amount of slip during each event was calculated from an empirical relationship between seismic moment ( $M_0$ ) and slip ( $d$ )<sup>35</sup>, where  $\log(d) = 0.17 \log(M_0) - 2.36$ . The scalar moment is calculated from magnitude using the relationship between magnitude and scalar seismic moment<sup>36</sup>. The slip rate between events can be obtained by dividing the amount of slip during the next similar earthquake by the recurrence interval according to the slip-predictable model<sup>37</sup>. If an expected previous or next event falls outside the analysis period, we extrapolated by using the lowest value of the average or adjacent slip rate. We assume that sequences occurring in almost the same location indicate aseismic slip in the same area. To display the spatial distribution of slip rates, we calculated the average slip rate and plotted this at the center of each similar earthquake pair. A total of 619 time series of slip rates were obtained in the present study. The list is provided in Supplementary Data 2. The average slip rate, relative plate motion, and their standard deviation in each subduction zone area were calculated from the slip rate for each group obtained here and the relative plate motion at their occurrence.

To track short-term variations, we use the method outlined in the previous section but also assume that the slip rate of each recurring similar earthquake is perturbed according to temporal changes observed in the regular seismic activity in adjacent regions. We calculated the short-term history of the slip rate by dividing the amount of slip in the next similar earthquake by the frequencies of nearby seismic events that occurred during the inter-seismic period of similar earthquake sequences. We selected seismic events with a magnitude of  $\geq 4.5$  and hypocentral distances of  $< 30$  km from each similar earthquake sequence. Both methods result in the same cumulative slip if the time window is sufficiently long compared with the recurrence interval of each similar earthquake sequence.

To investigate the long-term evolution of slip rate during the earthquake cycle, we calculated the slip rate against the elapsed time since the 11 megathrust earthquakes with  $M_w \geq 8.3$  that occurred after 1923. The list is provided in Supplementary Table 1. As of 2016, 93 years have elapsed since the oldest megathrust event occurred. We first calculated the slip rates in each plate boundary area smoothed using a 3-year moving average and normalized by the plate convergence rate in the area (pink bars in Fig. 4). Then, the time series for the same period were stacked (red bars in Fig. 4). With the information on the time series of slip rates, we outlined the long-term evolution of slip rate (blue curve in Fig. 4). The curve between 10 and 30 years of the time elapsed from megathrust rupture is somewhat uncertain due to the lack of data. To fill this gap, it is required to track the time-series of slip rate using similar earthquake sequences within the next decades.

## Data availability

Seismic waveform data used in this study are available from the Data Management Center of the National Research Institute for Earth Science and Disaster Resilience (NIED)<sup>38,39</sup> (<https://hinetwww11.bosai.go.jp/auth/?LANG=en>), the Japan Meteorological Agency (JMA) ([http://www.data.jma.go.jp/svd/eqev/data/bulletin/index\\_e.html](http://www.data.jma.go.jp/svd/eqev/data/bulletin/index_e.html)), [http://www.data.jma.go.jp/svd/eqev/data/daily\\_map/index.html](http://www.data.jma.go.jp/svd/eqev/data/daily_map/index.html), and the Earthquake Research Institute, the University of Tokyo (<http://tkypub.eri.u-tokyo.ac.jp/harvest>). The hypocenter catalog used in this study is available from the United States Geological Survey (<http://earthquake.usgs.gov/earthquakes/search>). Additional data related to this paper are available in Supplementary Data 1, Supplementary Data 2, and Supplementary Information.

## Code availability

The Generic Mapping Tools<sup>40</sup> created figures are obtained from <https://www.generic-mapping-tools.org/>. The analysis codes used in this study are available from the corresponding author upon request.

Received: 17 August 2020; Accepted: 15 February 2021;

Published online: 19 March 2021

## References

- Peng, Z. & Gomberg, J. An integrated perspective of the continuum between earthquakes and slow-slip phenomena. *Nat. Geosci.* **3**, 599–607 (2010).
- Obara, K. & Kato, A. Connecting slow earthquakes to huge earthquakes. *Science* **353**, 253–257 (2016).
- Igarashi, T., Matsuzawa, T. & Hasegawa, A. Repeating earthquakes and interplate aseismic slip in the northeastern Japan subduction zone. *J. Geophys. Res. Solid Earth* <https://doi.org/10.1029/2002JB001920> (2003).
- Igarashi, T. Spatial changes of inter-plate coupling inferred from sequences of small repeating earthquakes in Japan. *Geophys. Res. Lett.* <https://doi.org/10.1029/2010GL044609> (2010).
- Igarashi, T. Catalog of small repeating earthquakes for the Japanese Islands. *Earth Planets Space* <https://doi.org/10.1186/s40623-020-01205-2> (2020).
- Zhang, J., Richards, P. G. & Schaff, D. P. Wide-scale detection of earthquake waveform doublets and further evidence for inner core super-rotation. *Geophys. J. Int.* <https://doi.org/10.1111/j.1365-246X.2008.03856.x> (2008).
- Yu, W. Shallow-focus repeating earthquakes in the Tonga-Kermadec-Vanuatu subduction zones. *Bull. Seismol. Soc. Am.* <https://doi.org/10.1785/0120120123> (2013).
- Yu, W., Song, T.-R. A. & Silver, P. G. Repeating aftershocks of the great 2004 Sumatra and 2005 Nias earthquakes. *J. Asian Earth Sci.* <https://doi.org/10.1016/j.jseas.2013.02.018> (2013).
- Kato, A. & Nakagawa, S. Multiple slow-slip events during a foreshock sequence of the 2014 Iquique, Chile Mw 8.1 earthquake. *Geophys. Res. Lett.* <https://doi.org/10.1002/2014GL061138> (2014).
- Meng, L., Huang, H., Burgmann, R., Ampuero, J. P. & Strader, A. Dual megathrust slip behaviors of the 2014 Iquique earthquake sequence. *Earth Planet. Sci. Lett.* **411**, 177–187 (2015).
- Chen, K. H., Nadeau, R. M. & Rau, R.-J. Towards a universal rule on the recurrence interval scaling of repeating earthquakes? *Geophys. Res. Lett.* **34**, L16308 (2007).
- Nadeau, R. M., Foxall, W. & McEvilly, T. V. Clustering and periodic recurrence of microearthquakes on the San Andreas fault at Parkfield, California. *Science* **267**, 503–507 (1995).
- Slunga, R., Rognvaldsson, S. T. & Bodvarsson, R. Absolute and relative locations of similar events with application to microearthquakes in southern Iceland. *Geophys. J. Int.* **123**, 409–419 (1995).
- Schaff, D. P. & Richards, P. G. Repeating seismic events in China. *Science* <https://doi.org/10.1126/science.1093422> (2004).
- Ferretti, G., Massa, M., & Solarino, S. An improved method for the recognition of seismic families: application to the Garfagnana-Lunigiana area, Italy. *Bull. Seismol. Soc. Am.* <https://doi.org/10.1785/0120040078> (2005).
- Li, L., Chen, Q.-F., Cheng, X. & Niu, F. Spatial clustering and repeating of seismic events observed along the 1976 Tangshan fault, north China. *Geophys. Res. Lett.* **34**, L23309 (2007).
- Li, L., Chen, Q., Niu, F. & Su, J. Deep slip rates along the Longmen Shan fault zone estimated from repeating microearthquakes. *J. Geophys. Res. Solid Earth* **116**, B09310 (2011).
- Schaff, D. P. & Richards, P. G. On finding and using repeating seismic events in and near China. *J. Geophys. Res. Solid Earth* **116**, B03309 (2011).
- Zoet, L. K., Anandakrishnan, S., Alley, R. B., Nyblade, A. A. & Wiens, D. A. Motion of an Antarctic glacier by repeated tidally modulated earthquakes. *Nat. Geosci.* <https://doi.org/10.1038/ngeo1555> (2012).
- Naoi, M. et al. Unexpectedly frequent occurrence of very small repeating earthquakes ( $-5.1 \leq M_w \leq -3.6$ ) in a South African gold mine: implications for monitoring intraplate faults. *J. Geophys. Res. Solid Earth* <https://doi.org/10.1002/2015JB012447> (2015).
- Yu, W. & Wen, L. Deep-focus repeating earthquakes in the Tonga-Fiji subduction zone. *Bull. Seismol. Soc. Am.* <https://doi.org/10.1785/0120110272> (2012).
- Rubinstein, J. L., Uchida, N. & Beroza, G. C. Seismic velocity reductions caused by the 2003 Tokachi-Oki earthquake. *J. Geophys. Res. Solid Earth* **112**, B05315 (2007).
- Tkalčić, H., Young, M., Bodin, T., Ngo, S. & Sambridge, M. The shuffling rotation of the Earth's inner core revealed by earthquake doublets. *Nat. Geosci.* <https://doi.org/10.1038/NNGEO01813> (2013).
- Argus, D. F., Gordon, R. G. & DeMets, C. Geologically current motion of 56 plate relative to the no-net-rotation reference frame. *Geochemistry Geophys. Geosystems* **12**, Q11001 (2011).
- Uchida, N., Asano, Y. & Hasegawa, A. Acceleration of regional plate subduction beneath Kanto, Japan, after the 2011 Tohoku-oki earthquake. *Geophys. Res. Lett.* <https://doi.org/10.1002/2016GL070298> (2016).
- Kogan, M. G. et al. The mechanism of postseismic deformation triggered by the 2006–2007 great Kuril earthquakes. *Geophys. Res. Lett.* **38**, L06304 (2011).
- Gunawan, E. et al. A comprehensive model of postseismic deformation of the 2004 Sumatra–Andaman earthquake deduced from GPS observations in northern Sumatra. *J. Asian Earth Sci.* <https://doi.org/10.1016/j.jseas.2014.03.016> (2014).
- Freed, A. M. et al. Resolving depth-dependent subduction zone viscosity and afterslip from postseismic displacements following the 2011 Tohoku-oki, Japan

- earthquake, *Earth Planet. Sci. Lett.* <https://doi.org/10.1016/j.epsl.2016.11.040> (2017).
29. Ozawa, S. et al. Preceding, coseismic, and postseismic slips of the 2011 Tohoku earthquake, Japan. *J. Geophys. Res. Solid Earth* <https://doi.org/10.1029/2011JB009120> (2012).
  30. Mavrommatis, A. P., Segall, P. & Johnson, K. M. A decadal-scale deformation transient prior to the 2011 Mw 9.0 Tohoku-oki earthquake. *Geophys. Res. Lett.* <https://doi.org/10.1002/2014GL060139> (2014).
  31. Kato, A. et al. Propagation of slow slip leading up to the 2011 Mw 9.0 Tohoku-Oki earthquake. *Science* <https://doi.org/10.1126/science.1215141> (2012).
  32. Hori, T. & Miyazaki, S. A possible mechanism of M9 earthquake generation cycles in the area of repeating M7~8 earthquakes surrounded by aseismic sliding. *Earth Planets Space* <https://doi.org/10.5047/eps.2011.06.022> (2011).
  33. Aster, R. C. & Scott, J. Comprehensive characterization of waveform similarity in microearthquake data sets. *Bull. Seismol. Soc. Am.* **83**, 1307–1314 (1993).
  34. Menke, W., Lerner-Lam, A. L., Dubendorff, B. & Pacheco, J. Polarization and coherence of 5 to 30 Hz seismic wave fields at a hard-rock site and their relevance to velocity heterogeneities in the crust. *Bull. Seismol. Soc. Am.* **80**, 430–449 (1990).
  35. Nadeau, R. M. & Johnson, L. R. Seismological studies at Parkfield VI: moment release rates and estimates of source parameters for small repeating earthquakes. *Bull. Seismol. Soc. Am.* **88**, 790–814 (1998).
  36. Hanks, T. C. & Kanamori, H. A moment magnitude scale. *J. Geophys. Res. Solid Earth* **84**, 2348–2350 (1979).
  37. Shimazaki, K. & Nakata, T. Time-predictable model for large earthquakes. *Geophys. Res. Lett.* **7**, 279–282 (1980).
  38. National Research Institute for Earth Science and Disaster Resilience. NIED Hi-net. *National Research Institute for Earth Science and Disaster Resilience* <https://doi.org/10.17598/NIED.0003> (2019).
  39. National Research Institute for Earth Science and Disaster Resilience. NIED F-net. *National Research Institute for Earth Science and Disaster Resilience* <https://doi.org/10.17598/NIED.0004> (2019).
  40. Wessel, P. et al. The generic mapping tools version 6. *Geochemistry Geophys. Geosystems* <https://doi.org/10.1029/2019GC008515> (2019).

## Acknowledgements

We thank the National Research Institute for Earth Science and Disaster Resilience (NIED) and the Japan Meteorological Agency (JMA) for allowing us to use waveform data from their telemetric stations. We also used hypocenter catalogs from the United

States Geological Survey. This work supported by the Ministry of Education, Culture, Sports, Science and Technology (MEXT) of Japan, under its Earthquake and Volcano Hazards Observation and Research Program.

## Author contributions

T.I. conceived the study and conducted the data analysis. T.I. and A.K. contributed to the interpretation of the results and the manuscript preparation.

## Competing interests

The authors declare no competing interests.

## Additional information

**Supplementary information** The online version contains supplementary material available at <https://doi.org/10.1038/s43247-021-00127-5>.

**Correspondence** and requests for materials should be addressed to T.I.

**Peer review information** Primary handling editor: Joe Aslin.

**Reprints and permission information** is available at <http://www.nature.com/reprints>

**Publisher's note** Springer Nature remains neutral with regard to jurisdictional claims in published maps and institutional affiliations.



**Open Access** This article is licensed under a Creative Commons Attribution 4.0 International License, which permits use, sharing, adaptation, distribution and reproduction in any medium or format, as long as you give appropriate credit to the original author(s) and the source, provide a link to the Creative Commons license, and indicate if changes were made. The images or other third party material in this article are included in the article's Creative Commons license, unless indicated otherwise in a credit line to the material. If material is not included in the article's Creative Commons license and your intended use is not permitted by statutory regulation or exceeds the permitted use, you will need to obtain permission directly from the copyright holder. To view a copy of this license, visit <http://creativecommons.org/licenses/by/4.0/>.

© The Author(s) 2021, corrected publication 2021